ORIGINAL PAPER

High-Temperature Oxidation Behaviour of a TiAl-Based Alloy Subjected to Aluminium Hot-Dipping

D. Pilone[1] ◻ · **A. Mondal**[1] ◻ · **L. Zortea**[1] ◻

Abstract

In this research the oxidation resistance at high temperature of a TiAl-based alloy has been improved by hot-dipping the alloy in molten aluminium and by performing an interdiffusion process. After selecting the best process parameters, a compact $TiAl_3$ coating characterized by an almost constant thickness was formed on the surface. Isothermal oxidation tests, carried out at 900, 950 and 1000 °C, showed that the coated alloy is able to form a continuous and thin alumina layer that is very protective. Microstructural investigations highlighted that, above 900 °C, long residence times at high temperature determine the diffusion through the $TiAl_3$ layer of Cr that favours migration toward the outer surface of Al and thus the formation of a self-healing alumina layer.

Graphical Abstract
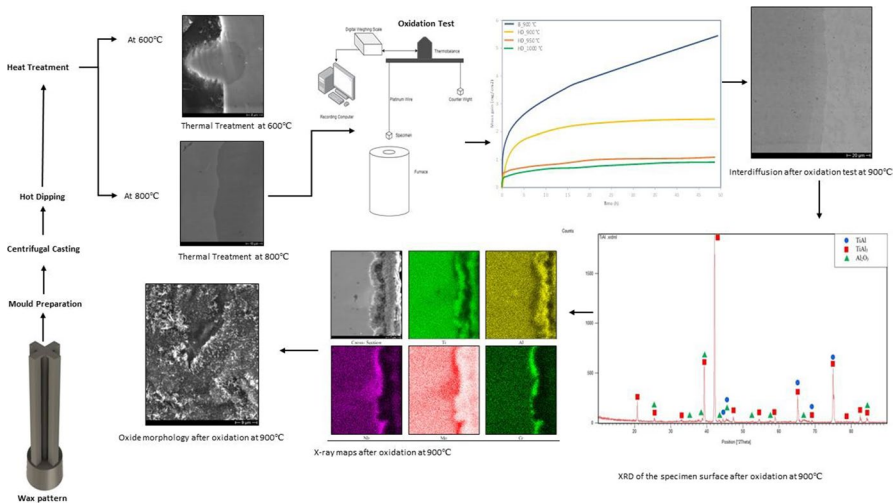
Extended author information available on the last page of the article

Introduction

TiAl intermetallic alloys have been deeply studied over the last few decades because of their high specific mechanical properties and their interesting properties for high-temperature applications [1, 2]. Economic and environmental stringent requirements for aviation have forced manufacturers to raise the engine temperature and to reduce weight. TiAl alloys are the best candidates for these applications because they have mechanical properties at high temperature comparable to those of Ni superalloys, but they are characterized by half of their weight. There are several factors that influence the possibility of increasing the number of TiAl applications. The development of an affordable processing method that allows to produce homogeneous and sound components is the first step. In addition to that, tailoring the alloy composition to increase fracture toughness at room temperature and mechanical properties at high temperature is very important [3]. Considering that these alloys are interesting candidates for high-temperature applications, one of the key issues is to increase the oxidation resistance at temperatures higher than 800 °C [4–6]. Fundamental studies on the oxidation behaviour of TiAl intermetallic alloys have been carried out starting from the end of 1980. The basic studies [7, 8] highlighted that at high-temperature TiAl intermetallics form different types of oxide with a layered structure containing Al_2O_3 and TiO_2. The oxide scale formed on these alloys reaches a critical thickness above which there is breakaway oxidation. Research works revealed that the composition and then the behaviour of the scale are affected by the alloy composition, the gas composition and the service temperature. Other critical aspects of these alloys at high temperature are the formation of voids at the metal-oxide interface and the formation in the alloy of an Al-depleted layer that becomes very brittle due to its high oxygen solubility. Over the years, many studies have been carried out to improve the oxidation resistance of these alloys by adding selected alloying elements. In fact, oxidation resistance can be improved by modifying the alloy compositions, particularly by the addition of Mo, W, and Nb. The "doping effect" [9] seems to determine the suppression of TiO_2 growth. The hypothesis to explain this phenomenon is that when ions with valence $+5$ or $+6$, such as Nb and W, are incorporated in the scale, oxygen vacancies are reduced with consequent suppression of TiO_2 growth. Many experimental works highlighted the beneficial effect of Nb on the alloy oxidation behaviour [10–12]. Rare earths could also improve high-temperature oxidation resistance because they not only promotes selective oxidation of Al, but also promote, like in other alloys, the formation of pegs anchoring the oxide layer to the metallic substrate. [13–15]

In order to improve the oxidation behaviour at high temperatures many researchers followed the surface modification route. One of the commonly used methods is thermal diffusion performed by favouring the diffusion of alloying elements, such as Al, Nb, Si and Mo from the surface. Al is the most interesting element because it is able to enrich only the external layer of the material and to promote the formation at high

temperatures of an adherent protective layer of alumina. Analysis of the literature highlights that pack aluminizing is the most used method [16–18]. The drawbacks of this method are the limited size of the components that can be treated and the fact that the aluminium-rich layer easily cracks as a result of the mismatch between substrate and coating. Ion implantation is another method used to increase oxidation resistance: it is performed at room temperature and almost all elements can be implanted on the surface. However, its limit is that its thickness is very small, and then the long term oxidation protection is very poor [19].

Laser surface alloying has been used for many years to create a coating layer on the surface of Ti and TiAl alloys with good results [20, 21] but there are still problems that need to be solved, in fact this process produces gas defects due to the use of a shielding gas and cracks due to the high cooling rates that produce relevant residual stresses.

The aim of this work is to study the effect of a hot-dip aluminised layer on the high-temperature oxidation resistance of a TiAl intermetallic-based alloy. Few attempts of applying this method [22, 23] have been made to form an Al-rich layer on TiAl alloys and Ti substrates [24]. In this research, a process has been set up to obtain an aluminium-rich layer having a constant thickness and without irregularities or cracks.

Experimental Procedures

The specimens used in this experimental work were produced using investment casting. A wax pattern was prepared by using five wax specimens (4.5×4.5×55 mm) connected to a riser as shown in Fig. 1. The riser is conical in shape to facilitate the metal flow. Once the model was completed, a ceramic material that does not react with the alloying elements was selected as the mould material. The mould was created by placing the wax model in the centre of a tube and filling it with the ceramic slurry. After filling, this was left to dry and solidify at room temperature for 24 h. Once dried, the wax pattern was melted by heating it in an oven at 150 °C for 2 h. The mould was then put in a furnace for thermal treatment as follows:

1. Heating the mould from room temperature to 250 °C and maintaining this temperature for 30 min.
2. Heating from 250 to 900 °C and staying there for 30 min.
3. Cooling the mould back to 450 °C.

The casting was performed using pure Ti, Al, Cr, Nb, and Mo. The elements were placed in a crucible made of a refractory material and melted in a centrifugal induction furnace under vacuum after five argon washing cycles. After melting, the molten metal was cast directly into the mould using the same centrifugal casting furnace. The mould

Fig. 1 Drawing of the wax pattern

was then put back in the furnace at 450 °C for 3 h for residual stress relieving. After cooling at room temperature the mould was broken and the casting was extracted. The casting was then cut to obtain the specimens used for the tests. Samples from each casting were ground using SiC papers ranging from 80 to 2400 grit, polished with 0.1 μm alumina suspension, and then etched with Keller's reagent to observe the microstructure by using the optical microscope.

The cut specimens had a rough surface, hence they were ground using SiC paper from 80 to 600 grit. For the hot-dipping process pure aluminium was melted in an open furnace and maintained at 800 °C. Before hot-dipping, the samples were etched in a solution containing 5% HF and 10% HNO_3 for 25 s. The specimens were then dried using a hot air blower. After drying, the specimens were immersed in the molten aluminium for 25 s and then slowly removed. They were then air-cooled to room temperature. Once cooled, the specimens were then heat treated to promote the interdiffusion process.

Isothermal oxidation tests were carried out in air using a thermobalance at 900 °C, 950 °C and 1000 °C. The mass gain was recorded by a computer. A weighing scale was attached to the thermobalance that measured the instantaneous mass of the specimen and sent it to the computer (Fig. 2). The computer recorded the mass gain of the sample at an interval of 300 s for 48 h.

The samples, after isothermal oxidation tests, were sectioned to analyse the element distribution in both the oxide scale and the base alloy by means of SEM/EDS. The morphology and composition of the oxide layer were studied by performing SEM analyses and x-ray diffraction with Cu k-α source. XRD measurements were made with a Philips PW 1830 diffractometer equipped with a Philips X'PERT vertical Bragg–Brentano powder goniometer. A step–scan mode was used in the 2θ range from 10° to 90° with a step width of 0.02° and a counting time of 1 s per step. The radiation used was the monochromatic Cu Kα radiation.

Results and Discussion

Although all of the specimens had the same nominal composition, they were slightly different in composition after casting. The average atomic composition of the alloy, obtained by performing EDS analyses on several samples, can be seen in Table 1.

Figure 3 shows the alloy microstructure characterised by lamellar colonies of α_2/γ phases and γ grains.

Preliminary tests were performed to optimise the hot-dipping process. These tests revealed that the best results were obtained by using an etching solution containing 5% HF and 10% HNO_3 and by performing the etching for 25 s. After the hot-dipping process in molten aluminium, few of the specimens were cut in order to observe the TiAl-Al interface. As can be seen in Fig. 4, right after hot-dipping, there is good adherence between the aluminium and the base alloy. Afterwards, to promote interdiffusion the specimens were subjected to different heat treatments.
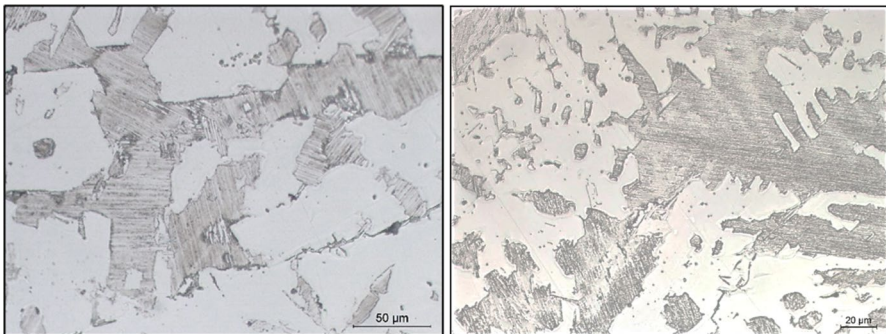
For this study, two different temperatures were selected for the interdiffusion treatment:
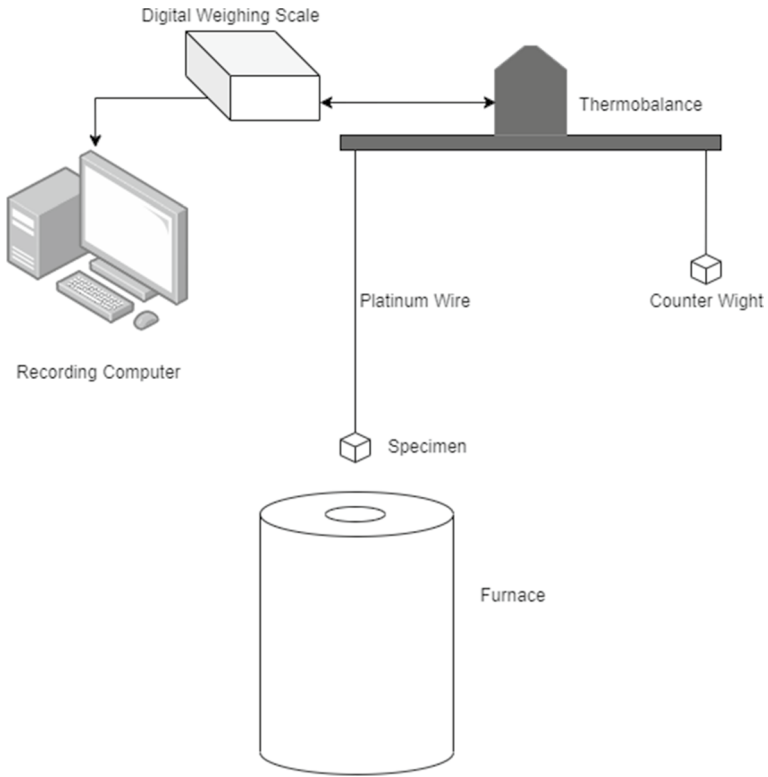
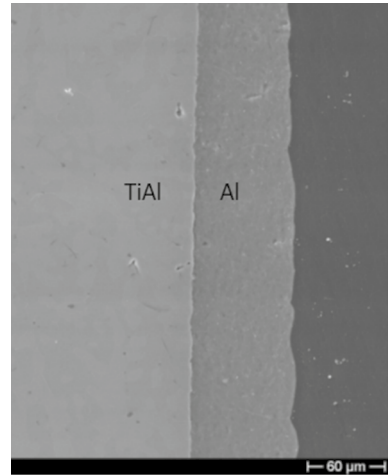**Fig. 2** Schematic representation of oxidation test set up

Table 1 Mean composition of the TiAl-based alloy used for the tests

Elements	Ti	Al	Cr	Nb	Mo
Atomic %	43.5	49.5	3.9	1.5	1.6

**Fig. 3** Optical micrographs showing the TiAl-based alloy microstructure

Fig. 4 Optical micrographs
showing the adherence between
metallic substrate and Al after
hot-dipping

1. A temperature below the melting temperature of aluminium: 600 °C for 3 h.
2. A temperature above the melting temperature of aluminium: 800 °C for 3 h.

SEM observation of the sections of the specimens treated at 600 °C highlighted that the interdiffusion did happen but it was not continuous along the interface. As it can be observed in Fig. 5 an intermetallic phase due to the interdiffusion process was locally formed, but only in limited areas. The formed phase was rich in aluminium ($TiAl_3$) as verified by the EDS analyses (Fig. 5).

The heat treatment carried out at 800 °C allowed to form, after 3 h, a continuous interdiffusion layer as it can be seen in Fig. 6. Semiquantitative EDS analyses performed on the superficial layer suggest that this layer is constituted by $TiAl_3$.
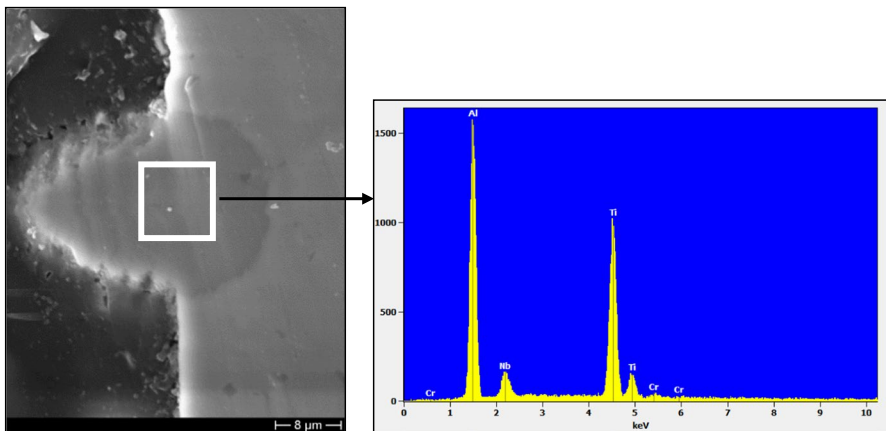
Fig. 5 SEM micrograph showing one of the interdiffusion areas after thermal treatment at 600 °C for 3 h and, on the right side, the EDS spectrum of this area

Fig. 6 SEM micrograph showing the intermetallic layer formed on the surface of the specimens after hot-dipping and after thermal treatment at 800 °C for 3 h
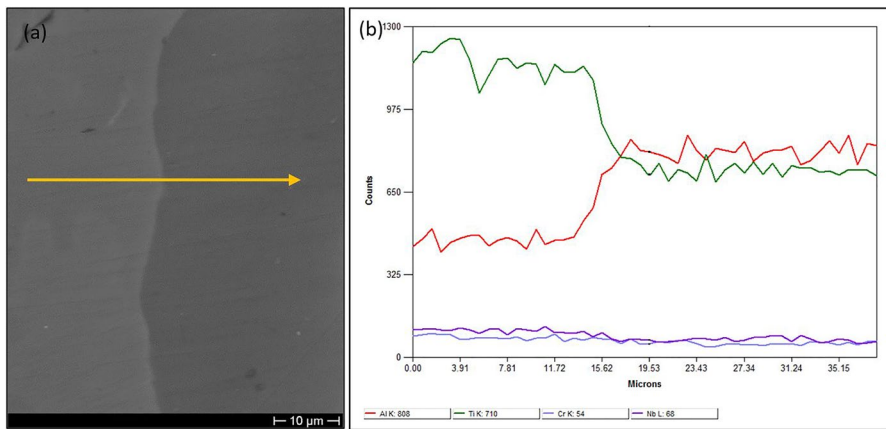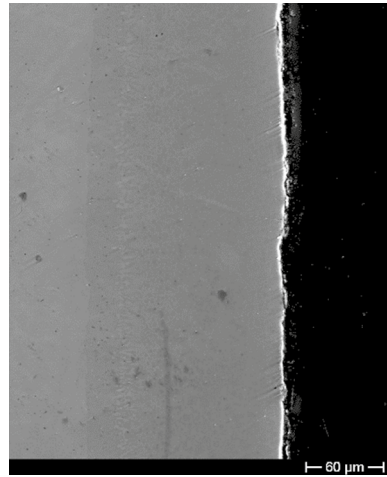

Fig. 7 SEM micrograph **a** showing the interface between TiAl base alloy and $TiAl_3$ intermetallic layer formed after thermal treatment at 800 °C for 3 h. The line analysis **b** highlights the element distribution in this area

A line analysis performed on the specimen section (Fig. 7) shows that, after heat treatment, the interdiffusion layer formed is an aluminium-rich intermetallic. Hence, this temperature was the one selected for obtaining the Al-rich coating layer. It is well known from the literature that the $TiAl_3$ intermetallic alloy is able to produce on its surface at high temperature a layer of alumina and that this layer becomes even more protective in presence of particular alloying elements [25, 26]. It must also be highlighted that by using hot-dip aluminising and interdiffusion at 800 °C it is possible to form a continuous layer of $TiAl_3$. This layer does not show the presence of cracks that characterize the aluminium-rich layer formed on TiAl by pack aluminising as described in the literature [16–18].

Once heat treated, the specimens were then subjected to isothermal oxidation tests to study the oxidation kinetics. The curves reported in Fig. 8 show that at 900 °C the mass gain reaches approximately 2.2 mg/cm². Isothermal oxidation tests carried out at 950 and 1000 °C highlighted that the mass gain decreases reaching a value of about 0.8–1 mg/cm². This is probably due to the fact that, by increasing the temperature, aluminium diffusion towards the surface is favoured with respect to the diffusion of other alloying elements. By comparing these values with the mass gain of the bare alloy, it is apparent that at 900 °C the mass gain of the alloy not subjected to hot-dipping is about 5.4 mg/cm² after 48 h and that the oxide layer formed is not very protective: in fact, the isothermal oxidation curve at 900 °C does not have a horizontal asymptote. On the contrary, the oxidation curves of the alloy after hot-dipping in molten aluminium show that, at each temperature, the treated alloy is able to form a compact, thin and very adherent alumina layer that efficiently protects the substrate alloy.

The study of the high-temperature oxidation controlled by the diffusion of reactive species through the oxide scale and/or through the subjacent alloy can be performed by evaluating the overall oxidation kinetics. Diffusion-driven oxidation processes generally produce parabolic kinetics described by the parabolic law $\Delta m^2 = k_\mathrm{p} t$, where Δm is the mass gain per unit area and k_p is the parabolic rate constant. As far as the behaviour of the tested alloy at 900 °C is concerned, the bare alloy exhibits a parabolic rate constant of $6.8\ 10^{-4}$ mg² cm⁻⁴ s⁻¹ in the first 2 h of oxidation while after hot-dipping and interdiffusion treatment the parabolic rate constant become lower reaching a value of $2.2\ 10^{-4}$ mg² cm⁻⁴ s⁻¹. By increasing the oxidation temperature up to 950 °C the parabolic rate constant become $2.7\ 10^{-5}$
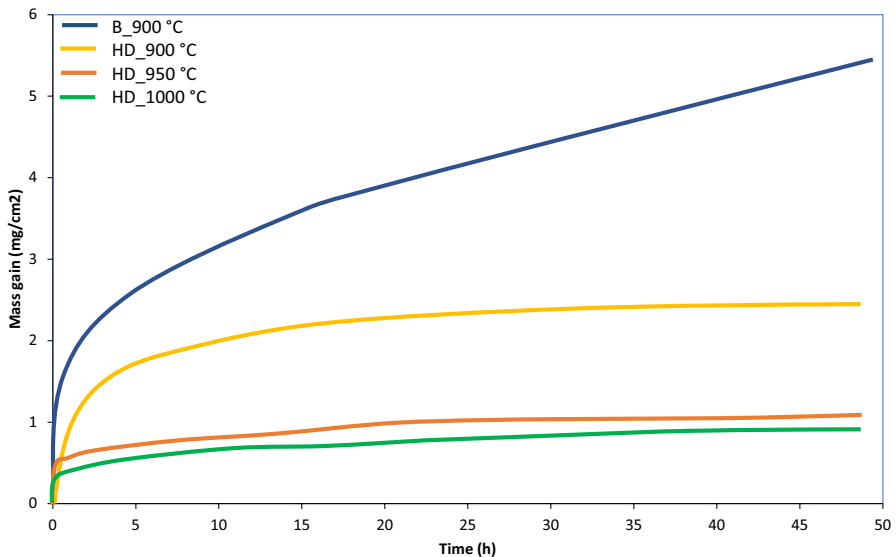
Fig. 8 Isothermal oxidation curves of the bare alloy at 900 °C (B_900 °C) and of the specimens, after hot-dipping and interdiffusion treatment, tested at 900, 950 and 1000 °C (HD_900 °C, HD_950 °C and HD_1000 °C)

$\text{mg}^2 \text{ cm}^{-4} \text{ s}^{-1}$: this is probably due to the fact that by increasing the temperature Al diffusion towards the surface is favoured with respect to Ti diffusion and the alumina layer formed determines a lower oxygen diffusivity. As it can be observed from Fig. 8 the alloy protected by the $TiAl_3$ coating is able to produce, after 1/2 h of test, a very protective oxide layer. The experimental curves obey the parabolic law only in the first 20 min since after that time interval the oxide layer becomes very protective and the weight gain remains almost constant.

After isothermal oxidation tests, the cross sections of the specimens were observed to analyse possible changes in the base material/aluminium-rich coating interface and in order to study the oxide composition and morphology. Close observation of the micrograph in Fig. 9 reveals that at the oxidation test temperature of 900 °C an intermediate phase ($TiAl_2$) is formed at the interface between the coating and the substrate. Literature data reveal that the diffusivity of Al (D_{Al}) and Ti (D_{Ti}) in the TiAl phase are $2 \times 10^{-18} \text{ m}^2\text{s}^{-1}$ and $1.1 \times 10^{-17} \text{ m}^2\text{s}^{-1}$, respectively [27]. This suggests that the outward diffusion of Ti from the substrate would be an order of magnitude higher than the inward diffusion of Al from the coating to the substrate. Therefore, there is an enrichment of Ti and a depletion of Al at the substrate/coating interface that, with time, will produce intermediate phases such as $TiAl_2$ (Fig. 9).

After the oxidation test, the specimens were also subjected to an XRD test to identify the phases present in the alloy surface after oxidation. The XRD pattern (Fig. 10) shows that the main phases in the alloy after oxidation are Al_2O_3 and $TiAl_3$: then a thin layer of Al_2O_3 is produced on the $TiAl_3$ substrate formed after the interdiffusion process.

The cross sections of the specimens were also subjected to EDS analyses and the obtained x-ray maps show the distribution of different elements in the specimen section (Fig. 11). The observation of this figure reveals that a phase rich in Cr, Mo, and Nb is formed just beneath the oxide layer. During oxidation tests chromium, niobium and molybdenum do not diffuse concurrently with Al and Ti in the outward direction from the bulk alloy, but remain predominantly in the metallic substrate,
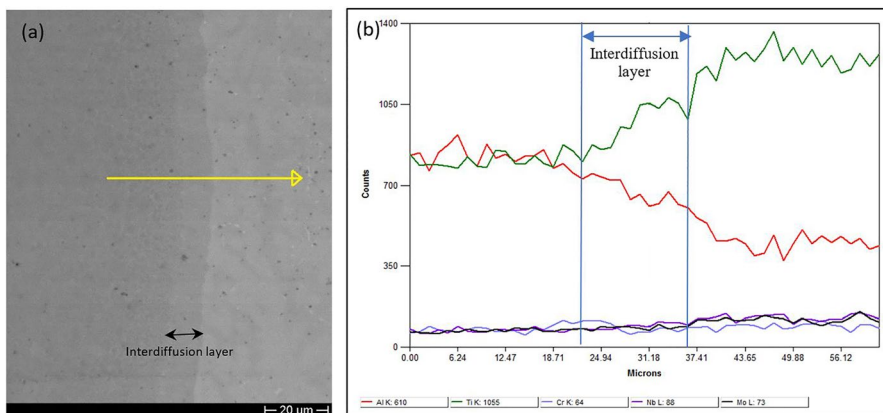

Fig. 9 SEM micrograph **a** showing the interdiffusion area after isothermal oxidation test at 900 °C and the line analysis **b** that shows element distribution
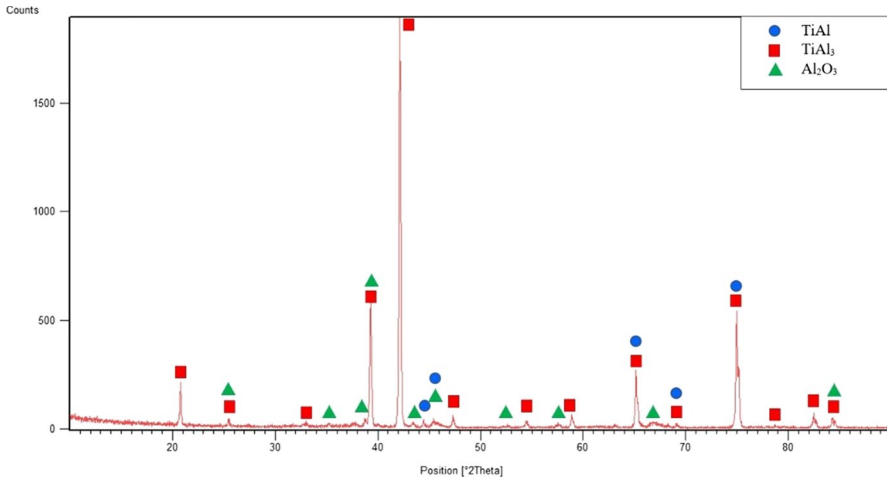
Fig. 10 XRD pattern of the surface of the specimen after hot-dipping, interdiffusion treatment and oxidation at 900 °C for 48 h

where they concentrate, forming a new phase beneath the oxide layer. The presence of this phase could affect Al and Ti migration towards the surface.

Figure 11 shows that the oxide layer is few micrometres thick and contains Al_2O_3 and TiO_2. If we compare this section with the one of the bare alloy subjected to oxidation at 900 °C, it is apparent that the oxide layer formed on the bare alloy, which has a thickness of about 20 μm, is constituted by alternating layers of TiO_2 and Al_2O_3 (Fig. 12) that are not miscible, as well known from the literature concerning TiAl-based alloys [7]. EDS analyses and x-ray maps show areas that consist mainly of either Ti and O or Al and O. In combination with XRD analyses these areas very likely consist of TiO_2 and Al_2O_3, respectively. A careful observation of x-ray maps highlights also that the TiO_2 layers are doped with Nb that, due to its doping effect, hinders the oxygen diffusion through the oxide layer and thus improves the oxidation resistance of the alloy. The presence of alternating layers of TiO_2 and Al_2O_3 makes the oxide scale less protective, as shown by the isothermal oxidation tests. This porous oxide layer tends to spall off during cooling to room temperature. XRD pattern reported in Fig. 13 confirms that the oxide layer is constituted by a mix of Ti and Al oxides. In Fig. 8 it can also be observed that, above 900 °C, the alloy after hot-dipping and interdiffusion treatment shows a very protective behaviour. Figure 14 shows the section of the hot-dip aluminised specimen after interdiffusion treatment and isothermal oxidation test at 950 °C. As expected the oxide layer is about 2 μm-thick and it is constituted by a continuous alumina layer adherent to the $TiAl_3$ layer. By observing the x-ray maps reported in Fig. 14 it is apparent that at 950 °C Cr is able to diffuse through the $TiAl_3$ layer forming phases that are able to promote at high temperature the preferential diffusion of aluminium towards the external surface. This phenomenon is able to determine a very good oxidation resistance due to the formation of a protective and self-healing alumina layer. At 1000 °C oxidation kinetics and alloy behaviour are very similar to those observed at 950 °C.
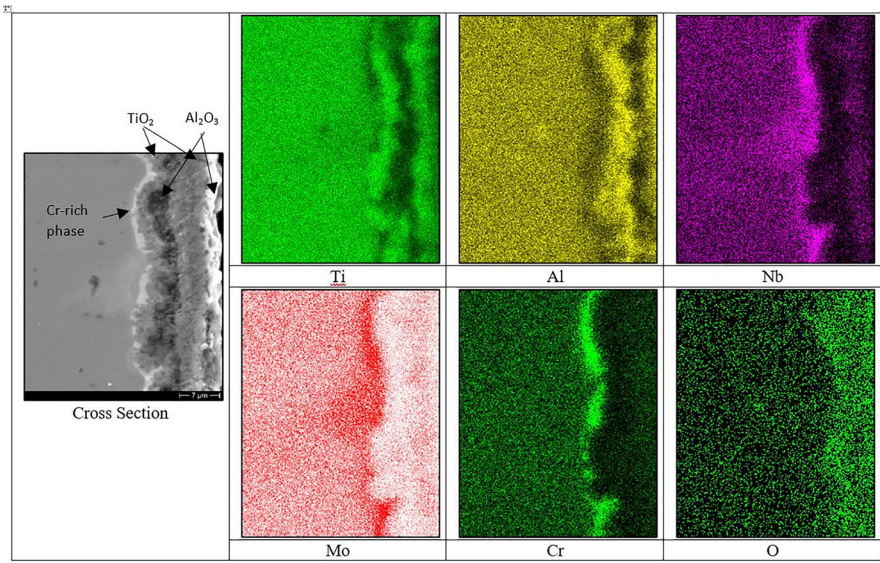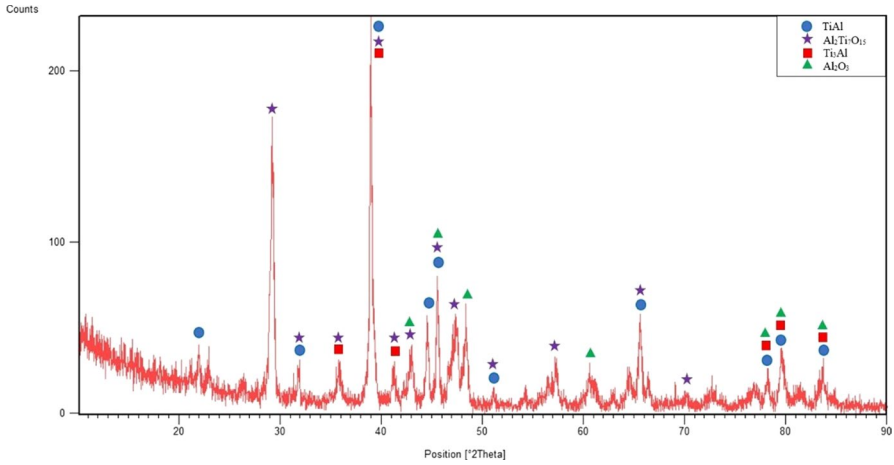
Fig. 11 X-ray maps showing the element distribution on the section of a hot-dipped specimen after isothermal oxidation test carried out at 900 °C for 48 h

In order to have more information about the behaviour of the specimens at high temperature the oxide morphology has been studied. The presence on the specimen surface of either Al_2O_3 or TiO_2 can easily be identified, not only by EDS
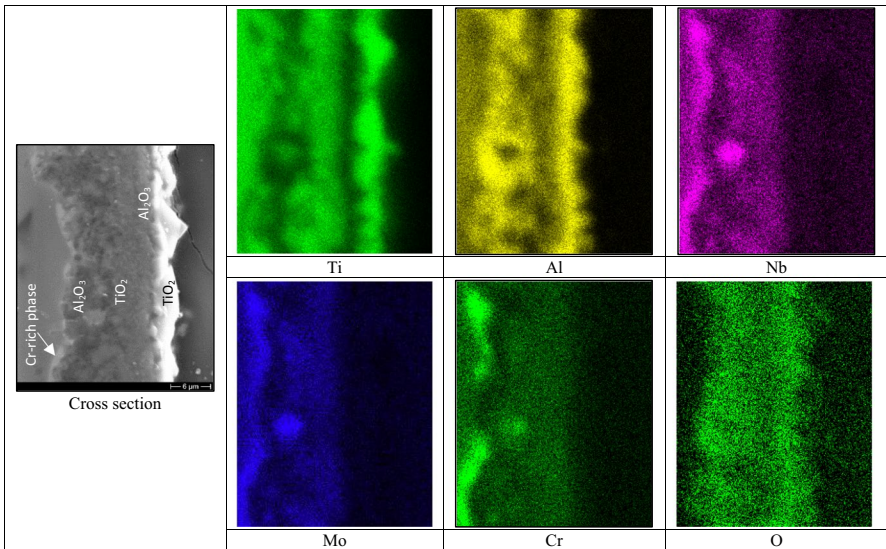
Fig. 12 X-ray maps showing the element distribution on the section of a specimen of the bare alloy after isothermal oxidation test carried out at 900 °C for 48 h

Fig. 13 XRD pattern of the surface of the specimen not subjected to hot-dipping after oxidation at 900 °C for 48 h
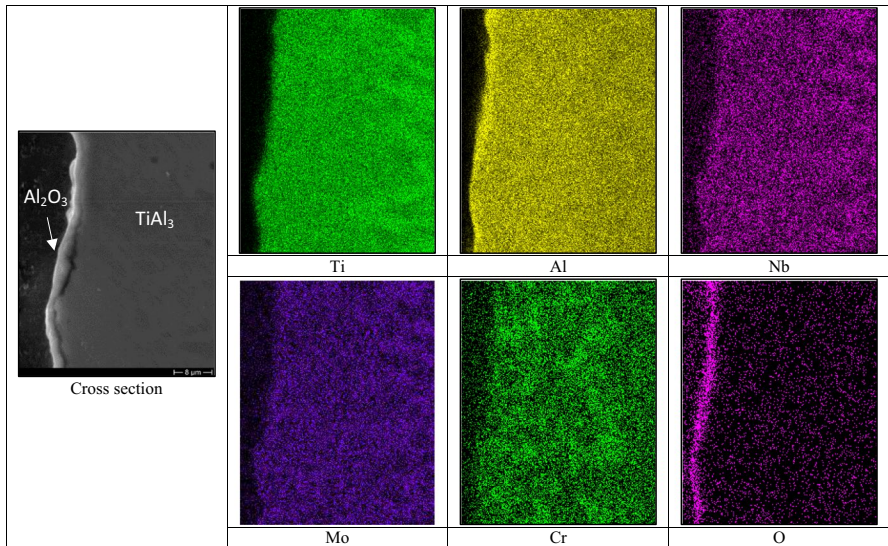
Fig. 14 X-ray maps showing the element distribution on the section of a hot-dipped specimen after isothermal oxidation test carried out at 950 °C for 48 h

analyses, but also by observing the oxide morphology: while Al_2O_3 has a needle-like morphology, TiO_2 is characterised by polyhedric crystals. In Fig. 15a, it is evident that after hot-dipping and interdiffusion treatment at 800 °C the surface is covered by an outermost alumina layer that has a very fine acicular structure
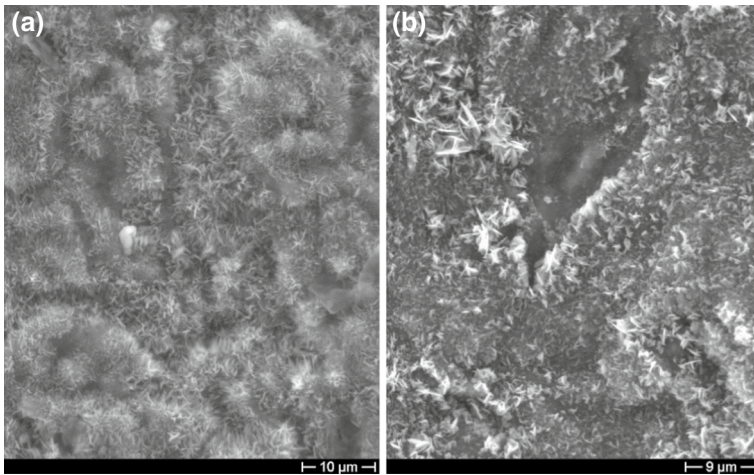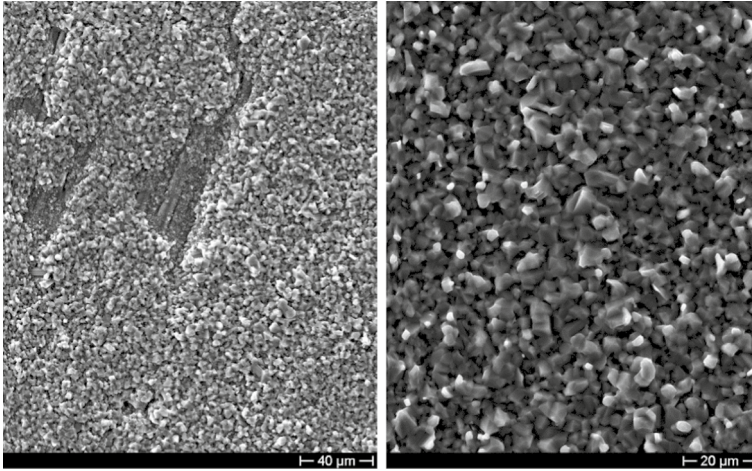
Fig. 15 SEM micrograph showing **a** the oxide morphology after interdiffusion treatment at 800 °C and **b** the oxide morphology after isothermal oxidation treatment carried out at 900 °C for 48 h

characterised by ripples. Figure 15b shows, after isothermal oxidation test at 900 °C a very similar oxide morphology. From the literature, it is well known that when the alumina scale grows due to inward oxygen transport, it appears flat since the new oxide is formed almost exclusively at the metal/oxide interface [28]. In contrast, when there is a mixed transport mode of aluminium and oxygen, new oxide is formed within the scale and thus this mechanism produces oxide convolutions [28].

By observing the morphology of the oxide grown on the surface of the bare alloy after oxidation tests at 900 °C (Fig. 16), it can be noticed that the alloy forms on the external surface the typical TiO_2 polyhedric crystals. In some areas (Fig. 16a) the outermost TiO_2 layer spalls off showing the underlying surface characterized by tiny alumina needles.

Conclusions

The experimental results highlighted that the hot-dipping of a TiAl-based alloy in molten aluminium improves the oxidation behaviour at high temperatures of the alloy. A careful selection of hot-dipping and interdiffusion process parameters allowed to obtain a compact and continuous $TiAl_3$ coating. Isothermal oxidation tests, carried out over the temperature range 900–1000 °C, revealed that the coated alloy produces at high temperature a continuous alumina layer that at 1000 °C limits, after 48 h test, the mass gain to about 0.8 mg/cm^2.

Fig. 16 SEM micrographs showing two images of the oxide morphology after 48 h isothermal oxidation test at 900 °C of a specimen not subjected to hot-dipping

Declarations

Conflict of interest The authors have no competing interests to declare that are relevant to the content of this article.

References

1. P. Janschek, Wrought TiAl blades. in *Materials Today: Proceedings*, Vol. 2 (Elsevier Ltd, 2015), pp. S92–S97.
2. X. Wu, *Intermetallics* **14**, 1114 (2006).
3. A. Brotzu, F. Felli, and D. Pilone, *Intermetallics* **54**, 176 (2014).
4. P. L. Narayana, J. H. Kim, D. W. Yun, et al., *Intermetallics* **141**, 107424 (2022).
5. J. Dai, J. Zhu, C. Chen, and F. Weng, *Journal of Alloys and Compounds* **685**, 784 (2016).
6. Y. Garip, *Intermetallics* **127**, 106985 (2020).
7. A. Rahmel, W. J. Quadakkers, and M. Schutze, *Materials and Corrosion* **46**, 271 (1995).
8. G. H. Meier and F. S. Pettit, *Materials Science and Engineering: A* **153**, 548 (1992).
9. M. Yoshihara and Y. W. Kim, *Intermetallics* **13**, 952 (2005).

10. D. Li, G. Zhang, G. Lu, J. Wang, et al., *Corrosion Science* **177**, 108971 (2020).
11. D. Pilone and F. Felli, *Intermetallics* **26**, 36 (2012).
12. D. Pilone, F. Felli, and A. Brotzu, *Intermetallics* **43**, 131 (2013).
13. M. Hadi, O. Bayat, M. Meratian, et al., *Oxidation of Metals* **90**, 421 (2018).
14. Y. Wu, K. Hagihara, and Y. Umakoshi, *Intermetallics* **12**, 519 (2004).
15. L. V. Ramanathan, *Corrosion Science* **35**, 871 (1993).
16. L. Mengis, C. Oskay, A. Donchev, et al., *Surface and Coatings Technology* **406**, 126646 (2021).
17. M. Z. Alam, K. Y. Durgarao, M. Kumawat, et al., *Surface and Coatings Technology* **380**, 125071 (2019).
18. L. K. Wu, J. J. Wu, W. Y. Wu, et al., *Corrosion Science* **146**, 18 (2019).
19. S. Hui, Z. Zhang, J. Xiao, and G. Yuan, *Rare Metals (English Edition) (China)* **18**, 161 (1999).
20. X. Liu, L. Yu, and H. Wang, *Xiyou Jinshu Cailiao Yu Gongcheng/Rare Metal Materials and Engineering* **30**, 224 (2001).
21. X.-B. Liu and H.-M. Wang, *Zhongguo Jiguang/Chinese Journal of Lasers* **32**, 1143 (2005).
22. Z. G. Zhang, Y. J. Wang, L. J. Xiao, et al., *Corrosion Science* **64**, 137 (2012).
23. Z. G. Zhang, X. Teng, Y. L. Mao, et al., *Oxidation of Metals* **73**, 455 (2010).
24. W. Deqing, S. Ziyuan, and T. Yingli, *Applied Surface Science* **250**, 238 (2005).
25. J. L. Smialek and D. L. Humprey, *Scripta Metallurgica et Materialia* **26**, 1763 (1992).
26. J. L. Smialek, *Corrosion Science* **35**, 1199 (1993).
27. Y. Mishin and C. Herzig, *Acta Materialia* **48**, 589 (2000).
28. W. J. Quadakkers, J. Nicholls, and D. Naumenko et al., Factors Affecting Oxide Growth Rates and Lifetime of FeCrAl Alloys. in *Materials Aspects in Automotive Catalytic Converters* (John Wiley & Sons, Ltd, 2002), pp. 93–105.

Authors and Affiliations

D. Pilone[1] · **A. Mondal**[1] · **L. Zortea**[1]

✉ D. Pilone
daniela.pilone@uniroma1.it

1 Dipartimento ICMA, Sapienza Università di Roma, Via Eudossiana 18, 00184 Rome, Italy